ELECTROMOTION 2001
June 19-20, 2001
Bologna - ITALY

# CALCULATION OF THE MECHANICAL AND ACOUSTIC BEHAVIOUR OF A CLAW POLE ALTERNATOR IN DOUBLE AND SINGLE STAR CONNECTION

*C. Kaehler, G. Henneberger*

Department of Electrical Machines (IEM)
Aachen Institute of Technology (RWTH)
Germany

**Abstract – This paper compares the acoustic behaviour of a claw pole alternator with different connection types of the stator coils. The alternator has a pole pair number of $p = 6$ and 72 stator slots (number of slots per phase winding $q = 2$). While the geometry of the alternator stays identical, the connection type of the stator coils is switched between a single and a double star point. An acoustic calculation method is utilised for each connection type. This paper aims at calculating the differences in the magnetic forces as well as the oscillation of the harmonics leading to the acoustic output of each connection type.**

## I. Introduction

Synchronous claw pole alternators are used in automobiles for generation of electricity. They are fairly efficient over a wide speed range and are inexpensive when built in high numbered series production. Another optimisation aspect is the audible noise of these alternators. Especially in the low speed range ($n = 2000 - 4000$ RPM), when the thermo-dynamical noise of the engine and the alternator fan noise are still relatively low, the noise caused by the magnetic excited forces of the generator has to be investigated. Measurements and calculations on various alternators have shown, that the acoustic characteristics of alternators are directly influenced by their connection type [1]. Significant differences appear when the number of stator slots per phase winding amounts to $q = 2$ as in the investigated alternator, whose number of pole pairs total $p = 6$, leading to 72 stator teeth. Three different connection types have been calculated:

1. double star-point, where a six pulse rectifier bridge with 12 diodes is used (in the following named connection type **double**),

2. single star-point with a serial connection in between the two slot windings of each phase winding (named **serial**) and

3. single star-point, where only one of each two coils in a phase winding is driven by a current in order to compare the results to a generator with half the number of stator slots ($q = 1$) built in series production (named **single slot**).

In this paper, the reasons for the acoustic differences of the methods of connection are investigated using numerical simulations. The same models of the claw pole alternator are used for each step in the calculation process. Only in the magneto-static simulation of the first step, different current distributions are impressed into the FE model. These distributions are chosen in such a way that in each case nearly identical output of electrical power is established. The magnetic forces as well as the mechanical and acoustic behaviour of the methods of connection are calculated and compared.

## II. Calculation procedure

The calculation procedure has been presented in [2] for star-connected alternators and in [1] for delta-connection. This procedure can be split into three blocks: the magneto-static computations, leading to the magnetic forces on the stator metal, the structural-dynamic calculation of the relevant harmonics and the acoustic simulation of the generator.

### *A. Magneto-static calculation*

First, finite element computations (FE) of the magneto-static field of the claw pole alternator at each connection type at various speeds are executed on models of one pole pitch (Fig. 1). Since the modelling of the winding head for machines with the number of stator slots per phase winding $q > 1$ is very complicated, the model is simplified in these regions. All other magnetically relevant regions are modelled precisely. In each of the five models the rotor is rotated by an

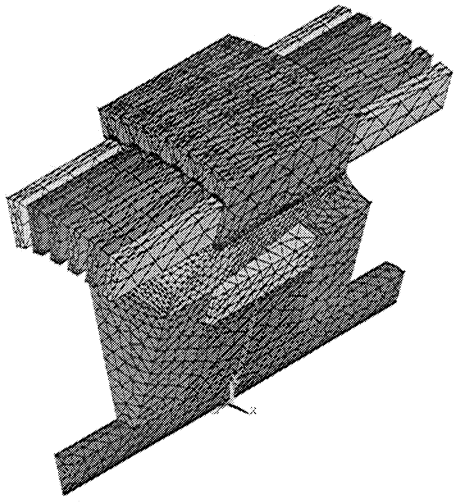

Fig. 1. Magnetic model, one pole pitch, simplified winding head

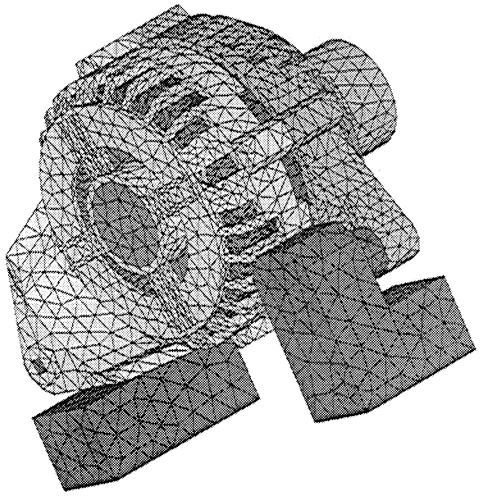

Fig. 2. Mechanical full 360° model

angle of:

$$\Delta\alpha = 2^o \cdot m \qquad \text{with} \qquad m \in \{0;1;2;3;4\}, \tag{1}$$

leading to five time steps.
An edge-based static FE solver as described in [3] is utilised for each time step. The solver is driven by a constant direct current in the rotor excitation coil. A three phase current is impressed into the stator coils. The current distribution in the stator depends on the connection type. Since in star-connections the higher harmonics of the stator currents can be neglected [1], only the base harmonic as represented in (2), (3) and (4) are used. For each phase winding two coil regions exist, which carry the following current values:

1. Connection type **double**:

$$\begin{aligned} I_1 &= \frac{1}{2} \cdot \hat{I} \cdot \sin(\omega t + \varphi + \Delta\alpha \cdot p + 15^o) \\ I_2 &= \frac{1}{2} \cdot \hat{I} \cdot \sin(\omega t + \varphi + \Delta\alpha \cdot p - 15^o) \end{aligned} \tag{2}$$

2. Connection type **serial**:

$$\begin{aligned} I_1 &= \frac{1}{2} \cdot \hat{I} \cdot \sin(\omega t + \varphi + \Delta\alpha \cdot p) \\ I_2 &= I_1 \end{aligned} \tag{3}$$

3. Connection type **single slot**:

$$\begin{aligned} I_1 &= \hat{I} \cdot \sin(\omega t + \varphi + \Delta\alpha \cdot p + 15^o) \\ I_2 &= 0.0 \end{aligned} \tag{4}$$

The amplitude of the current $\hat{I}$ and the load angle $\varphi$ are functions of the generator speed ($\omega$: angular velocity). In order to take saturation effects into account, they are determined in a model with $q = 1$ and compared to measurements [4].
The different excitations lead to variations in the flux density distribution. The magnetic forces are calculated in each static FE calculation based on the flux density distributions and the material data [5]:

$$\vec{\sigma} = \vec{n}_{12} \cdot [B_n \cdot (H_{1n} - H_{2n}) - (w_1' - w_2')]. \tag{5}$$

In (5) $\vec{n}_{12}$ represents the normal vector of the boundary between materials 1 and 2 (in this case stator iron and air). $B_n$ stands for the normal component of the flux density, $H_{1n}$ and $H_{2n}$ for the normal component of the magnetic field in material 1 and 2 and $w_1'$ and $w_2'$ stand for the magnetic coenergy densities of the materials.
For each connection type the forces at the five time steps are determined. Interpolation of different stator tooth positions leads to 30 time steps or 14 spectral modes for two tooth pitches [2].

### *B. Structural-dynamic computation*

The forces in spectral mode are transformed into a mechanical FE-model [6]. Since all mechanically relevant components have to be modelled, there is no symmetry and a full 360° model has to be generated (Fig. 2). This model is used to determine the deformation and oscillation of the relevant harmonics, based on the material data as obtained in [7]. Here, transversely isotropic materials are used to represent the stator metal sheets [8]. In order to reduce modelling and calculation expenses and since the rotor contributes barely to the acoustic outcome, the rotor region is modelled as a solid cylinder with the same mass as the claw-formed real-life rotor.
A node-based structural-dynamic FE solver is utilised for each relevant harmonic and alternator speed. The

solver's general equation of motion in finite element formulation reads [9]:

$$(\underline{K} + j \cdot \omega \cdot \underline{F} - \omega^2 \cdot \underline{M}) \cdot \vec{D} = \vec{R}. \quad (6)$$

In (6) $\underline{K}$ represents the stiffness matrix, $\underline{M}$ the mass matrix and $\underline{F}$ a damping factor. $\vec{R}$ stands for the external forces and $\vec{D}$ for the yet to be calculated deformations, while $\omega$ sets the angular velocity of the calculated harmonic. To increase the numerical accuracy, second order elements are used in the displacement solver [9].
In the case of the claw pole alternator the relevant harmonics are acoustic orders 5 and 6 or mechanical orders 30 and 36. Since these two orders lead almost to the complete noise output, all other orders are neglected.

### C. Acoustic simulation

In the last step, the sound power level is calculated using an acoustic boundary element model (BE). This model differs geometrically from the mechanical model. Here, only the surface boundaries are meshed and the stator and rotor region is merged in order to reduce numerical errors in the acoustic BE method caused by small air gaps. Again a $360^o$ model is used. Onto this model, the surface velocities $v_n$ of the structural-dynamic calculations are interpolated [9]:

$$v_n = \omega \cdot \vec{D} \cdot \vec{n}^T, \quad (7)$$

where $\vec{n}^T$ stands for the transposed normal vector of the boundary element. These velocities are used to drive the acoustic BE solver, whose matrix system can be described as follows [10]:

$$\sum_{\kappa=1}^{K} \int_{S_\kappa} \left[ j\omega\rho v_n(y) u^* + p(y) \frac{\partial u^*}{\partial n} \right] dS(y) =$$

$$\begin{cases} p(x) & : \ x \in \Omega \\ p(x)/2 & : \ x \in S \\ 0 & : \ x \in O \end{cases} \quad \text{with} \quad u^* = \frac{e^{-jkr}}{4\pi r}. \quad (8)$$

Equation (8) describes the acoustical boundary element formulation for harmonic excitations and K elements at the surface $S_\kappa$, where $v_n(y)$ are the known surface velocities and $p$ is the sound pressure. $x$ are the coordinates in the space $\Omega$, $y$ are the coordinates on the surface $S$ and $O$ is the space within the surface. On a half spherical boundary area the emitted sound distribution and the total sound power are evaluated [2]. A sound reflection plane represents the lower half space.
Repeating this calculation chain for various generator speeds and the relevant harmonics leads to the sound power characteristic of the machine.

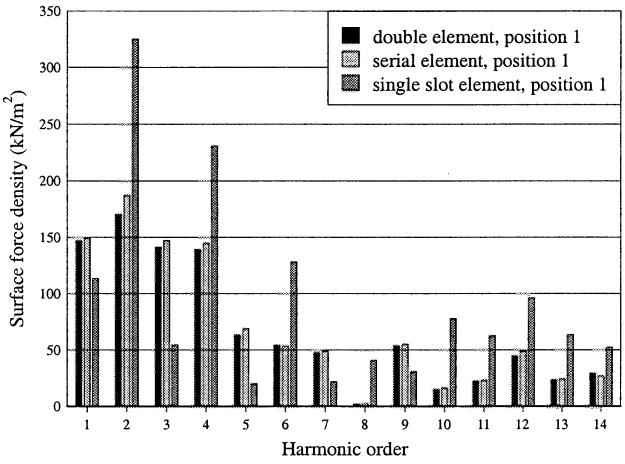


Fig. 3. Force density in spectral mode on primary tooth

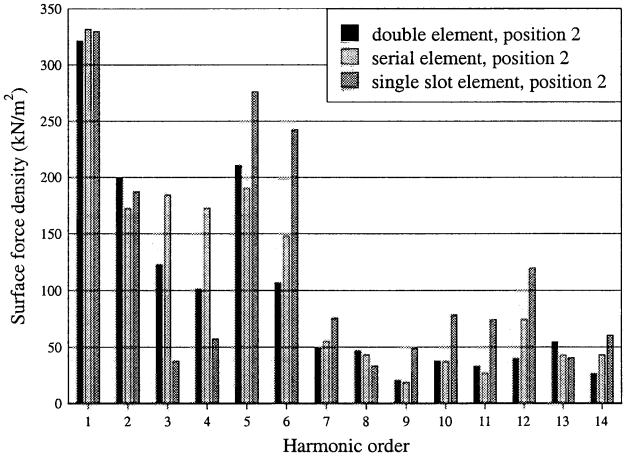


Fig. 4. Force density in spectral mode on secondary tooth

## III. Results

The results are separated again into the magnetic forces, the deformations and the acoustic sound power level. Different current distributions for all three connection methods lead to variations of the magnetic forces as well as the harmonics and distinguished sound power levels.

### A. Calculated force distribution

After the magnetic field is calculated, the forces on two stator teeth (one pole pitch) are determined for each connection type in time and spectral mode.
When comparing the surface force densities on specific elements of the stator tooth surface in spectral mode, differences between the two teeth of one stator pole pitch can be found. While on one of these teeth (here represented by position 1, Fig. 3) the even orders especially in **single slot** connection are elevated, on the second tooth the 5th and the 6th harmonic have

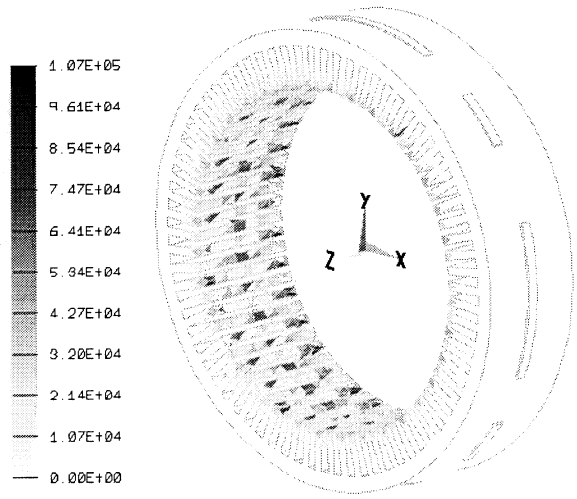


Fig. 5. Surface force density ($N/m^2$), real comp., **double**

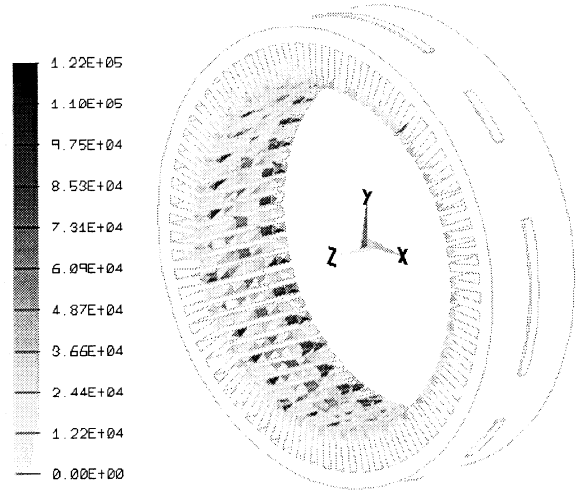


Fig. 6. Surface force density ($N/m^2$), real comp., **serial**

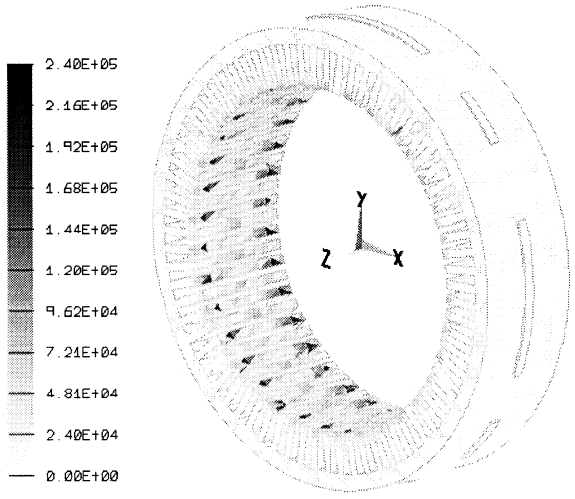


Fig. 7. Surface force density ($N/m^2$), real comp., **single slot**

Table I
Maximum force densities on stator teeth elements

| Connection type | real comp. | imag. comp. |
|---|---|---|
| double, order 5 | 168 $kN/m^2$ | 172 $kN/m^2$ |
| serial, order 5 | 147 $kN/m^2$ | 151 $kN/m^2$ |
| single slot, order 5 | 407 $kN/m^2$ | 227 $kN/m^2$ |
| double, order 6 | 107 $kN/m^2$ | 93 $kN/m^2$ |
| serial, order 6 | 122 $kN/m^2$ | 131 $kN/m^2$ |
| single slot, order 6 | 240 $kN/m^2$ | 811 $kN/m^2$ |

increased (position 2, Fig. 4). The specific element positions chosen have their locus at the axial middle of a stator tooth.

After the transformation into spectral mode, the surface force densities of each investigated harmonic are extrapolated onto all stator teeth of the mechanical model.

The force distribution of the real component of harmonic order 6 on the stator teeth are depicted in Fig. 5, 6 and 7. This harmonic order acts on every second tooth of the stator. The locuses of the force maxima are at the outer end regions of the tooth ground (Fig. 7). The distributions do not differ relevantly between the connection types, although in connection type **serial** (Fig. 6) and **double** (Fig. 5) there are force maxima on the middle of some stator teeth.

The maximum force densities are depicted in Tab. I. The surface forces for connection type **single slot** and both harmonics are about factor 3 to 4 higher, while the level stays constant for both other types, with slightly lower maximum force densities for connection type **double** and harmonic order 6. For harmonic order 5 connection type **serial** has the lowest force density maxima.

### *B. Structural behaviour of the generator*

The acoustically relevant harmonics of the claw pole alternator are harmonic orders 5 and 6. Therefore, only these orders are calculated. The stator of the generator is fixed to the housing on the middle of the stator back. The housing has the highest influence on the noise radiation. Thus, the noise level of this specific machine reacts stronger to a rise in even orders, leading to oval modes [1].

Since these modes do not differ relevantly, the calculated deformations of the stator metal of connection type **double** and harmonic order 6 are shown in Fig. 8 and 9 scaled by a factor of $1 \cdot 10^7$. The only different mode for harmonic order 6 appears at the imaginary component of connection type **single slot**. Here, a triangular mode forms (Fig. 10).

When comparing harmonic order 5 for all connection types, no change of modes exists. Only the maximal deformation varies in dependence of the connection

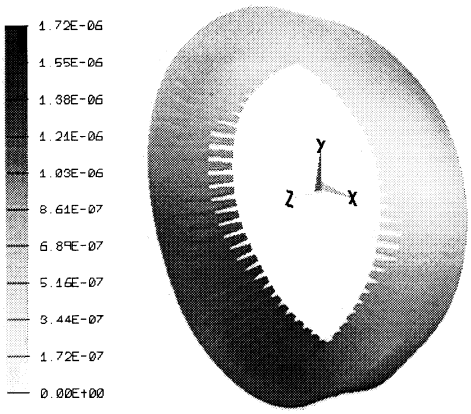


Fig. 8. Deformation (m), order 6, real comp., **double**

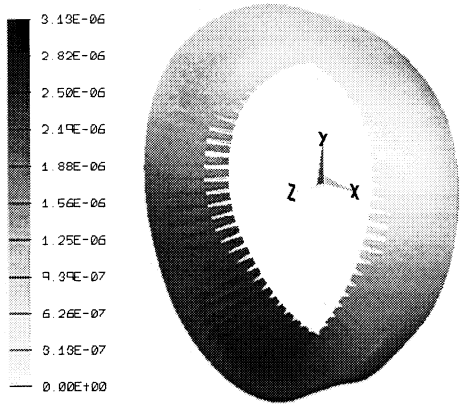


Fig. 9. Deformation (m), order 6, imaginary comp., **double**

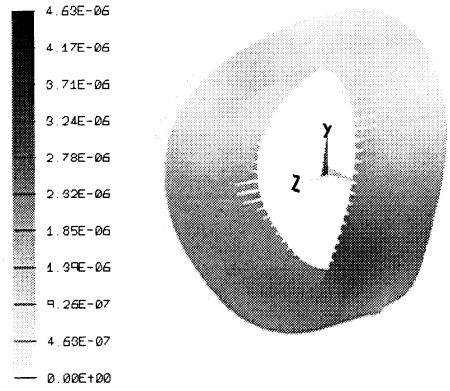


Fig. 10. Deformation (m), order 6, imag. comp., **single slot**

type. The modes can best be viewed for connection type **single slot** scaled by a factor of $5 \cdot 10^7$ as depicted in Fig. 11 and 12.

As in the force computations, the scale of the deformation values differ between the connection types as

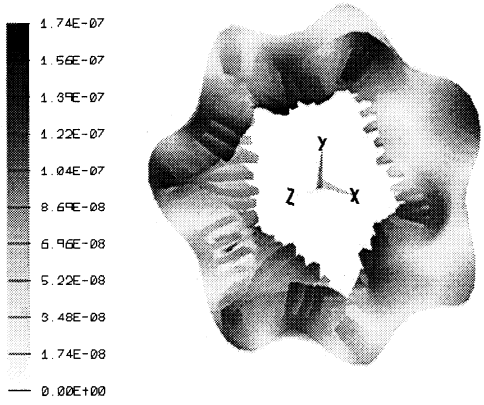


Fig. 11. Deformation (m), order 5, real comp., **single slot**

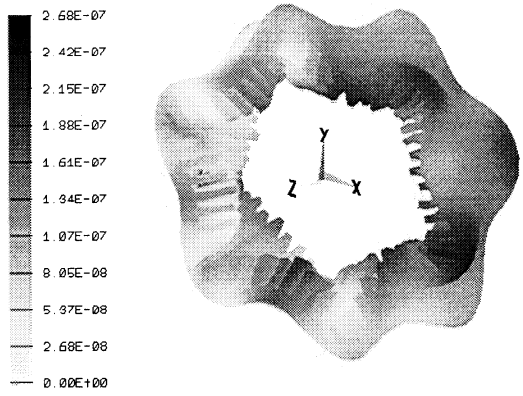


Fig. 12. Deformation (m), order 5, imag. comp., **single slot**

Table II
Maximum deformation of stator metal

| Connection type | real comp. | imag. comp. |
|---|---|---|
| double, order 5 | 73.9 nm | 116 nm |
| serial, order 5 | 93.2 nm | 93.2 nm |
| single slot, order 5 | 174 nm | 268 nm |
| double, order 6 | 1.72 $\mu$m | 3.13 $\mu$m |
| serial, order 6 | 2.66 $\mu$m | 4.88 $\mu$m |
| single slot, order 6 | 5.35 $\mu$m | 4.62 $\mu$m |

documented in Tab. II, which compares the maximum deformation values. Here again, connection type **single slot** is higher for harmonic order 5 than the other two types. For harmonic order 6 the maximum deformation of this connection type only causes the highest deformations for the real component.

### *C. Acoustic differences*

The calculated sound power levels of harmonic orders 5 and 6 and all connection types are depicted in Fig. 13 and 14 together with an alternator with $q = 1$. Due

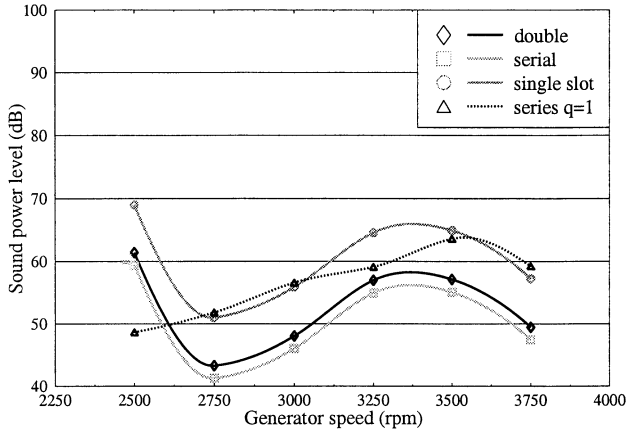


Fig. 13. Calculated sound power level of harmonic order 5

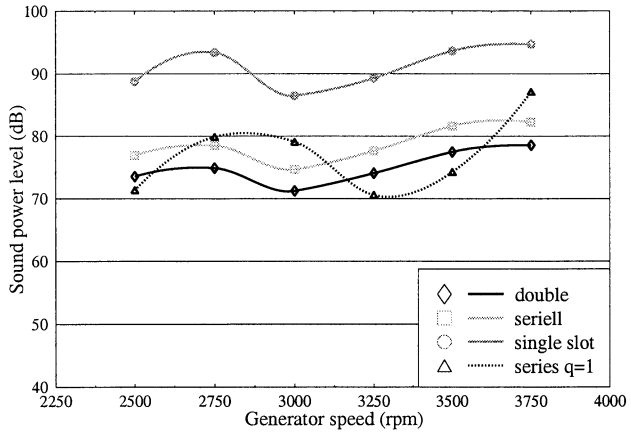


Fig. 14. Calculated sound power level of harmonic order 6

to the higher number of slots when $q = 2$, the stability of the stator metal is reduced and the resonance frequencies for harmonic order 6 appear at lower speed.

As expected, the larger oscillations and the different mode of harmonic order 6 in connection type **single slot** lead to a rise of the noise emission of about 10 dB over the whole speed spectrum (Fig. 14). The other two connection types differ by about 5 dB, which can again be derived form the lower deformations of connection type **double**. Both have about the same power level as the generator with $q = 1$.

The 5th order shows connection type **serial** by about 2 dB lower than connection type **double** (Fig. 13). Both connection types lie about 10 dB under connection type **single slot** and the alternator with $q = 1$, which shows no resonance behaviour at speed $n =$ 2500 RPM.

Since the sound levels of harmonic order 6 are over 20dB higher than harmonic order 5, the total noise output of harmonic order 6 can be taken as the alternator characteristic.

## IV. Conclusion

In this paper a comparison of three different connection types on a synchronous claw pole alternator is conducted. The presented results show a change in the force distributions of the stator surface forces. Here, the maximum force of the connection when only one of each two stator slots is driven by current (connection type **single slot**) is factor 3 to 4 higher than the other types. Consequently, this leads to higher oscillation amplitudes and higher noise output of this connection type. Since the forces of the double star-connection (**double**) are slightly lower than with a single star and serial connection (**serial**), it has the lowest noise radiation of all three connection types.

## V. References

[1] C. Kaehler and G. Henneberger, "Calculation of the differences in the acoustical behaviour of a claw-pole alternator when connected in delta and star," in *2nd International Seminar on Vibrations and Acoustic Noise of Electric Machinery*, (Lodz, Poland), pp. 127–131, VANEM, June 2000.

[2] I. Ramesohl, T. Bauer, and G. Henneberger, "Calculation procedure of the sound fields caused by magnetic excitations of the claw-pole alternator," in *1st International Seminar on Vibrations and Acoustic Noise of Electric Machinery*, (Bethune, France), pp. 75–79, VANEM, May 1998.

[3] D. Albertz and G. Henneberger, "On the use of the new edge based $\vec{A}, \vec{A} - \vec{T}$ formulation for the calculation of time-harmonic, stationary and transient current field problems," *IEEE Transactions on Magnetics*, vol. 36, pp. 818–822, July 2000.

[4] S. Küppers, *Numerische Verfahren zur Berechnung und Auslegung von Drehstrom- Klauenpolgeneratoren.* Aachen: Shaker Verlag, 1996. Dissertation, Institut für Elektrische Maschinen, RWTH Aachen.

[5] J. R. Melcher, *Continuum Electromechanics.* Cambridge Massachusetts: MIT Press, 1981.

[6] I. Ramesohl, C. Kaehler, and G. Henneberger, "Influencing factors on acoustical simulations including manufacturing tolerances and numerical strategies," in *9th International Conference on Electrical Machines and Drives*, (Canterbury, England), pp. 142–146, IEE EMD, September 1999. Conference Publication 468.

[7] I. Ramesohl and G. Henneberger, "Automatic structural material identification of electrical machines using the threshold accepting procedure," in *11th Conference on hte Calculation of Electromagnetic Fields*, (Rio de Janeiro, Brazil), pp. 555–556, COMPUMAG, November 1997.

[8] S. G. Lekhnitskii, *Anisotropic Plates.* New York, London, Paris: Gorden and Breach Science Publishers, 1956.

[9] I. Ramesohl and G. Henneberger, "Numerical calculation of the acoustic noise of claw pole alternators," in *Symposium on Coupled Magneto-Mechanical Problems*, (Gent, Belgium), May 1999.

[10] R. Ciskowski and C. Brebbia, *Boundary Element Methods in Acoustic.* Southampton Boston: Computational Mechanics Publication Elservier Applied Science, 1991.